

## Electronic Supporting Information

### The Fermi Level as an Energy Reference in Liquid Jet X-ray Photoelectron Spectroscopy

#### Studies of Aqueous Solutions

Lucía Pérez Ramírez<sup>a\*</sup>, Anthony Boucly<sup>a†</sup>, Florent Saudrais<sup>a‡</sup>, Fabrice Bournel<sup>ab</sup>, Jean-Jacques Gallet<sup>ab</sup>, Emmanuel Maisonhaute<sup>c</sup>, Aleksandar R. Milosavljević<sup>b</sup>, Christophe Nicolas<sup>b</sup> and François Rochet<sup>a\*</sup>.

<sup>a</sup> Sorbonne Université, CNRS, Laboratoire de Chimie Physique matière et Rayonnement, UMR 7614, 4 place Jussieu, 75005 Paris, France

<sup>b</sup> Synchrotron SOLEIL, L'Orme des Merisiers, Saint-Aubin - BP 4891192 Gif-sur-Yvette CEDEX, France

<sup>c</sup> Sorbonne Université, CNRS, Laboratoire Interfaces et Systèmes Electrochimiques, 4 place Jussieu, 75005 Paris, France

#### AUTHOR INFORMATION

##### Corresponding Author

\* francois.rochet@sorbonne-universite.fr

##### Present Addresses

♣ now at Sorbonne Université, CNRS (UMR 8234), Physicochimie des Electrolytes et Nanosystèmes Interfaciaux, 4 place Jussieu, 75252 Paris Cedex 05, France.

† now at Paul Scherrer Institute (PSI) Forschungsstrasse 111, 5232 Villigen, Switzerland.

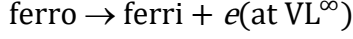
‡ now at Institut de Biologie Intégrative de la Cellule, Saclay Campus, CEA Saclay, 91191 Gif sur Yvette Cedex, France

Content: thermodynamics of the metal/solution interface; comment on the calculation of the SHE absolute potential; XPS spectrometer calibration; voltammetry and potentiometry; PHREEQC calculation; C 1s spectra; jet biasing; 0.1 M KCl solution spectra



## S1. A thermodynamic approach to the metal/redox solution interface

In the following we take the specific example of the  $\text{Fe}^{\text{III}}(\text{CN})_6^{3-}/\text{Fe}^{\text{II}}(\text{CN})_6^{4-}$  couple (in short the ferri/ferro couple) in water for which one electron is exchanged. First, we consider the oxidation reaction:



The energy of the electron at infinity (the vacuum level at infinity  $\text{VL}^\infty$ ) is zero. We consider the chemical potentials  $\mu_{\text{ferri}}^{\text{sol}}$ ,  $\mu_{\text{ferro}}^{\text{sol}}$  of the ferri and ferro species, respectively, in the aqueous solution (sol). For simplicity, the Hartree contribution  $q\phi_{\text{Hartree}}^{\text{sol}}$ , averaged over one unit cell of the metal,<sup>1</sup> or over a supercell consisting of several hundreds of molecules for water,<sup>2</sup> is incorporated into the chemical potential. By definition, the Gibbs energy difference of the oxidation reaction (expressed in eV/particle) is:

$$\Delta_r G_{\text{ferro/ferri}}^{\text{sol}} = \mu_{\text{ferri}}^{\text{sol}} - \mu_{\text{ferro}}^{\text{sol}} > 0. \quad \{1\}$$

Now we consider the thermodynamic equilibrium of the electroactive species in the solution with the metal electrode (met).



The electrochemical potentials of the ferricyanide (in the solution), of the ferrocyanide (in the solution) and of the electron in the metal are  $\tilde{\mu}_{\text{ferri}}^{\text{sol}}$ ,  $\tilde{\mu}_{\text{ferro}}^{\text{sol}}$ , and  $\tilde{\mu}_e^{\text{met}}$ , respectively. With  $\tilde{\mu}_e^{\text{met}} = \mu_e^{\text{met}} + qV_{\text{Galvani}}^{\text{met}}$ ,  $\tilde{\mu}_{\text{ferri}}^{\text{sol}} = \mu_{\text{ferri}}^{\text{sol}} + 3qV_{\text{Galvani}}^{\text{sol}}$  and  $\tilde{\mu}_{\text{ferro}}^{\text{sol}} = \mu_{\text{ferro}}^{\text{sol}} + 4qV_{\text{Galvani}}^{\text{sol}}$ , at equilibrium one gets:

$$\tilde{\mu}_e^{\text{met}} = \tilde{\mu}_{\text{ferro}}^{\text{sol}} - \tilde{\mu}_{\text{ferri}}^{\text{sol}} \quad \{2\}$$

The electric potential energies in the two phases will be no more be equal at equilibrium ( $qV_{\text{Galvani}}^{\text{met}} \neq qV_{\text{Galvani}}^{\text{sol}}$ ) to ensure the alignment of the electrochemical potentials following:

$$\mu_e^{\text{met}} + qV_{\text{Galvani}}^{\text{met}} = -\Delta_r G_{\text{ferro/ferri}}^{\text{sol}} + qV_{\text{Galvani}}^{\text{sol}} \quad \{3\}$$

We can set  $qV_{\text{Galvani}}^{\text{sol}}$  to zero with respect to the thermodynamic reference level, i.e. the electron at infinity ( $\text{VL}^\infty$ ), which to the equation that positions the common Fermi level (FL) with respect to the vacuum level at infinity ( $\text{VL}^\infty$ )

One finally gets:

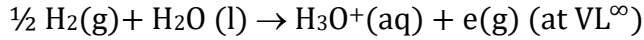
$$\text{VL}^\infty - \text{FL} = -\tilde{\mu}_e^{\text{met}} = \Delta_r G_{\text{ferro/ferri}}^{\text{sol}} \quad \{4\}$$

$\Delta_r G_{\text{ferro/ferri}}^{\text{sol}}$  is obtained by adding the measured electrode potential of the ferricyanide/ferrocyanide couple to the standard oxidation reaction Gibbs energy of the

reaction  $\frac{1}{2} \text{H}_2(\text{g}) + \text{H}_2\text{O}(\text{l}) \rightarrow \text{H}_3\text{O}^+(\text{aq}) + \text{e}(\text{g})$  (at  $\text{VL}^\infty$ ) (the absolute standard potential of  $\text{H}^+/\text{H}_2$  couple  $\Delta_r G_{\text{H}_2/\text{H}^+}^\ominus$ , see section S2).

## S2. Calculation of $\Delta_r G_{\text{H}_2/\text{H}^+}^\ominus$

Isse and Gennaro<sup>3</sup> calculate the standard Gibbs energy  $\Delta_r G_{\text{H}_2/\text{H}^+}^\ominus$  of the oxidation reaction



by adding the Gibbs formation energy of gas phase  $\text{H}^+$  to its Gibbs hydration energy, which is the correct way to obtain a SHE value based on the chemical potential (i.e. referred to  $\text{VL}^\infty$ ). The gas phase  $\text{H}^+$  Gibbs formation energy ( $1513.321 \text{ kJ}\cdot\text{mol}^{-1}/15.684 \text{ eV}$ ) is a well-established value. For its part, the  $\text{H}^+$  Gibbs hydration energy is calculated by Isse and Gennaro<sup>3</sup> ( $-1100.9 \text{ kJ}\cdot\text{mol}^{-1}/-11.41 \text{ eV}$ ) from ion-water cluster experiments by Coe and coworkers.<sup>4</sup> Expressed in eV/particle  $\Delta_r G_{\text{H}_2/\text{H}^+}^\ominus$  is  $4.281 \text{ eV}$ , considering  $\text{VL}^\infty$  as the reference.

## S2. Calibration of the XPS spectrometer and accuracy

The Fermi level of the XPS analyzer is determined using a gold wire (grounded as the analyzer) placed at the position of the liquid jet. The true photon energy is equal to the kinetic energy difference  $\text{KE}_{\text{Au } 4f_{7/2}}^a(2h\nu) - \text{KE}_{\text{Au } 4f_{7/2}}^a(h\nu)$  of the Au  $4f_{7/2}$  peak obtained with the first ( $h\nu$ ) and second diffraction order ( $2h\nu$ ) of the monochromator (see Figure S1). During the experimental run of 2019 (Zobell solutions and pure KCl solutions)  $h\nu$  was  $399.86(02) \text{ eV}$ . The binding energy of the Au  $4f_{7/2}$  peak  $\text{BE}_{\text{Au } 4f_{7/2}}$  with respect to the FL is  $83.95 \text{ eV}$  (see also ref. 5). Then the apparent analyzer work function  $\Phi_a$  is calculated from:

$$\Phi_a = h\nu - \text{BE}_{\text{Au } 4f_{7/2}} - \text{KE}_{\text{Au } 4f_{7/2}}^a \quad \{5\}$$

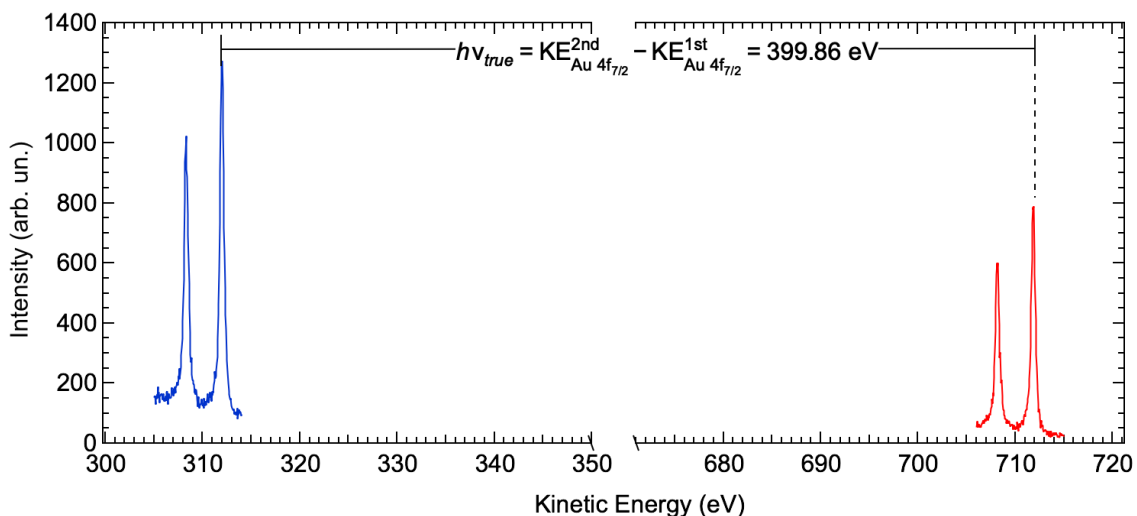


**Figure S1.** Determination of the true photon energy value using the Au 4f core-level measured at  $h\nu$  and  $2h\nu$ .

The results are given in Table S1 for the  $\text{FeCl}_3/\text{FeCl}_2$  run (run 1) and the Zobell run (run 2, 19 months after run 1). Over 19 months, the evolution of the calibration can appear small (less than 0.1 eV), but given the required accuracy, a calibration preceding each liquid jet run is needed.

| Pass energy (V) | Analyzer apparent work function $\Phi_a$ (eV) |                           |
|-----------------|---|---------------------------|
|                 | Precision $\pm 0.03$ eV                       |                           |
|                 | Run 1 $\text{FeCl}_3/\text{FeCl}_2$           | Run 2 (+19 months) Zobell |
| 100             | 2.81  | 2.84                      |
| 50              | 3.02  | 3.12                      |
| 20              | -   | 3.93                      |
| 10              | 3.36  | -                         |

**Table S1.** Calibration of the XPS spectrometer and evolution over 19 months.

BEs and work functions depend on the analyzer work function determination  $\pm 0.030$  eV, the photon energy  $\pm 0.020$  eV (Zobell/KCl run of 2019) and the fitting accuracy. Concerning the latter one, the SEEDC MP and HOMO centroid fitting give values to  $\pm 0.009$  eV and  $\pm 0.006$  eV, respectively. Therefore, BEs are known to  $\pm 0.056$  eV and work functions to  $\pm 0.060$  eV. The vertical IE is independent of the analyzer FL calibration, of the bias and depends only on

the precision on  $h\nu$  that is  $\pm 0.020$  eV (for run 2, Zobell solution), therefore, the total precision is  $\pm 0.035$  eV.

### S3. Cyclic voltammetry and potentiometry

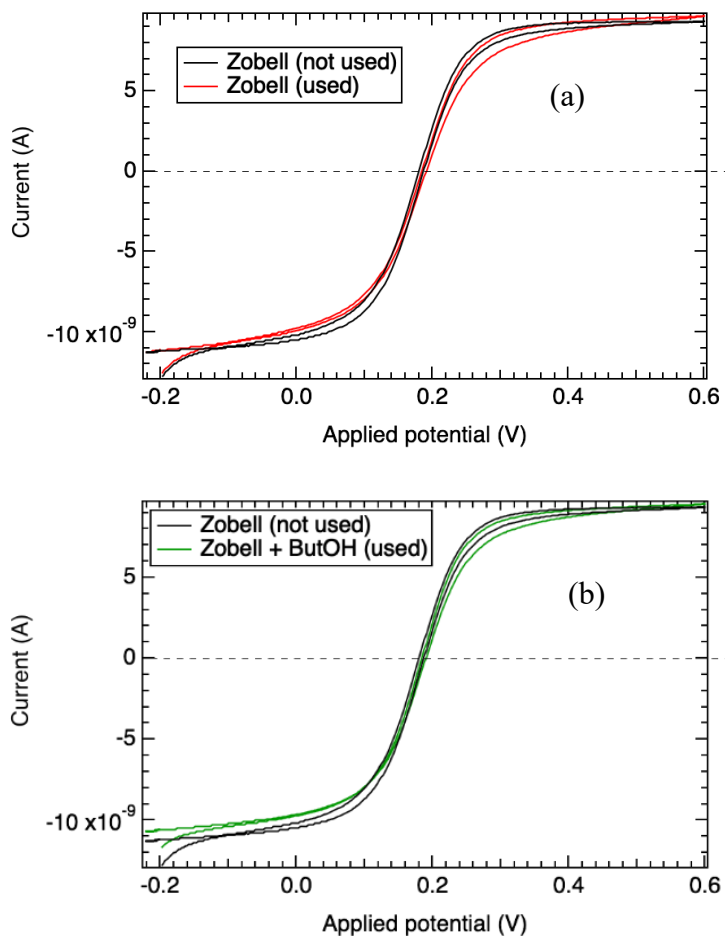


**Figure S2.** (a) voltammogram of the Zobell solution fresh (not used) and after exposure to the beam (used), (b) voltammogram of the Zobell solution plus 64 mM butanol fresh (not used) and after exposure to the beam (used). The reference is the standard calomel electrode. The measurements are made at 22°C.

The voltammogram of the Zobell solutions are shown in Figure S2 referenced to the standard calomel electrode. Useful parameters are collected in Table S2 They were acquired at  $10 \text{ mVs}^{-1}$  using a platinum ultramicroelectrode having a radius of  $12.5 \text{ }\mu\text{m}$ . In these

conditions, the cyclic voltammograms are steady states,<sup>6</sup> the limiting current  $I_l$  being expressed as:

$$I_l = 4nFDrC \quad \{6\}$$

With  $n$  the number of electrons exchanged ( $n = 1$  here),  $F$  the Faraday constant,  $D$  the diffusion coefficient,  $r$  the electrode radius and  $C$  the concentration. The current at  $I = 0$  corresponds to the open circuit potential (OCP). The OCP, limiting cathodic and anodic currents are given in Table S2. For the fresh solution (not exposed to the beam). The cathodic and anodic limiting currents are practically equal, which shows that the concentrations of ferrocyanide and ferricyanide are also practically equal (through equation {6}), as the diffusion coefficients are close ( $0.726(11) \times 10^{-5} \text{ cm}^2 \text{ s}^{-1}$  and  $0.667(14) \times 10^{-5} \text{ cm}^2 \text{ s}^{-1}$  for the ferricyanide and ferrocyanide at 25°C, respectively<sup>7</sup>).

For its part, the voltammogram of the Zobell solution exposed to the synchrotron beam is practically superposable to that of the fresh solution (Figure S2(a)). Considering the limiting currents and equation {6}, this shows that the concentrations of the ferricyanide and ferrocyanide ions has not changed appreciably. The unchanged OCP shows that no new couple due to water radiolysis is in sufficient concentration to create a mixed potential and alter the measurement.

Adding 1-butanol has not great effect on the voltammogram (Figure S2(b)). In particular, the OCP is unchanged. This explains why the (centroid) HOMO binding energies (see main article) are found at the same position.

| Solution               | Cathodic limiting current (A) | Anodic limiting current (A) | OCP SCE (V) | OCP SHE (V) |
|------------------------|-------------------------------|-----------------------------|-------------|-------------|
| Zobell (fresh)         | $9.29 \times 10^{-9}$         | $-1.13 \times 10^{-8}$      | 0.194       | 0.439       |
| Zobell (used)          | $9.30 \times 10^{-9}$         | $-1.13 \times 10^{-8}$      | 0.195       | 0.440       |
| Zobell + ButOH. (used) | $9.34 \times 10^{-9}$         | $-1.07 \times 10^{-8}$      | 0.195       | 0.440       |

**Table S2:** OCP of Zobell solutions fresh and after exposure (used) to the synchrotron beam. Measurements are made at 22°C. SCE: referenced to the standard calomel electrode. SHE: referenced to the standard hydrogen electrode.

Concerning the 50 mM FeCl<sub>3</sub>/ 50 mM FeCl<sub>2</sub> solution, the potentiometric measurements are reported in Table S3.

| 0.05 M FeCl <sub>3</sub> /0.05 M FeCl <sub>2</sub> | OCP SCE (V) | OCP SHE (V) |
|--|-------------|-------------|
| 1 min after fabrication                            | 0.478       | 0.723       |
| 10 min after fabrication                           | 0.475       | 0.720       |

**Table S3:** OCP measurement of the 0.05 M FeCl<sub>3</sub>/0.05 M FeCl<sub>2</sub> solution. Measurements are made at 22°C. SCE: referenced to the standard calomel electrode. SHE: referenced to the standard hydrogen electrode.

The PHREEQC program<sup>8</sup> was also used to calculate the composition of the 0.05 M FeCl<sub>3</sub>/0.05 M FeCl<sub>2</sub> solution, the pH and the SHE referenced electrode potential. Calculated values are reported in Table S4. Note that the dominant anionic species remains Cl<sup>-</sup>. The solution is acidic. The agreement with the potentiometry experiment (OCP) is excellent.

| 50 mM FeCl <sub>3</sub> /50 mM FeCl <sub>2</sub> Electrode potential (vs SHE) =0.715 V, pH=1.937 |                       |                        |                        |                        |                        |                                |                        |
|--|-----------------------|------------------------|------------------------|------------------------|------------------------|--------------------------------|------------------------|
| species  | H <sup>+</sup>        | Cl <sup>-</sup>        | FeCl <sup>2+</sup>     | FeCl <sup>+</sup>      | HCl                    | FeCl <sub>2</sub> <sup>+</sup> | FeCl <sub>2</sub>      |
| molality   | 1.44 10 <sup>-2</sup> | 2.537 10 <sup>-1</sup> | 2.788 10 <sup>-2</sup> | 2.043 10 <sup>-3</sup> | 3.349 10 <sup>-4</sup> | 2.470 10 <sup>-4</sup>         | 5.609 10 <sup>-6</sup> |

**Table S4:** PHREEQC program calculations

#### S.4 C 1s spectra

We show in Figure S3 (red curve) the C 1s peak of the Zobell solution. The photon energy is 674.29 eV. Therefore, the photoelectrons have a KE of ~380 eV, which corresponds to an electron attenuation length of ~2 nm.<sup>9</sup> The K<sup>+</sup> concentration is 0.1 M. At this concentration, the K 2p doublet is visible, appearing at 292.95 eV (2p<sub>3/2</sub>) and 295.77 eV (2p<sub>1/2</sub>) (binding energies are overestimated by 0.2 eV due to the streaming potential). Importantly, we note the absence of C 1s peak at ~285 eV, which proves the cleanliness of the jet (typical contaminants are fatty acids).

Upon addition of 64 mM 1-butanol, the C 1s spectrum (green curve) exhibits the characteristic lines of the alcohol, i.e., the alkyl carbons at ~284.9 eV, and the C-OH carbon at 286.4 eV. The ratio “alkyl C” to “C-OH” ratio corresponds to the stoichiometric ratio 3:1.

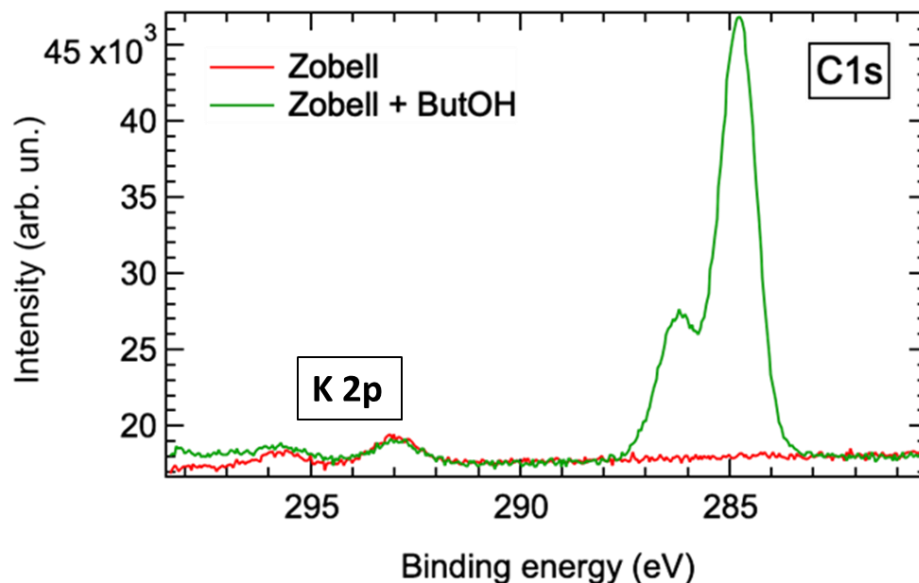


**Figure S3.** K 2p spectrum of the Zobell solution (red) and K 2p/ C 1s spectra of the Zobell + butanol solution (green). Binding energies are referenced to the FL of the analyzer/electrode. Binding energies are not corrected for the streaming potential that increases them by 0.2 eV (see main article). The photon energy is 674.29 eV.

### S5. Biasing the jet

We biased the 0.1 M KCl solution via the upstream electrode (the downstream catcher was biased at the same value) and we measured the corresponding O 1s spectra reported in Figure S4 (a). We used a photon energy of 673.74 eV and a pass energy of 50 eV. The kinetic energies are shifted by the differences in the nominal  $qV_{\text{bias}}$ . While the shape of the liquid phase HOMO peak remains unchanged, the peak at lower kinetic energy which corresponds to the gaseous water  $1b_1$  peak experiences an increasing broadening with increasing  $qV_{\text{bias}}$ . This phenomenon is due to the X-ray spot size that does not matching exactly the diameter of the liquid jet, so it ionizes (in addition to the jet) the gaseous water molecules between the liquid and the entrance to the analyzer. The Cl 2p spectra are shown in Figure S4 (b). The spectra were measured at a photon energy of 244.29 eV and a pass energy of 50 eV. The kinetic energies are also shifted by the differences in the nominal  $qV_{\text{bias}}$ . The Cl 2p spectra are aligned and do not exhibit any deformation as expected for the core-level of an element pertaining to the solution.

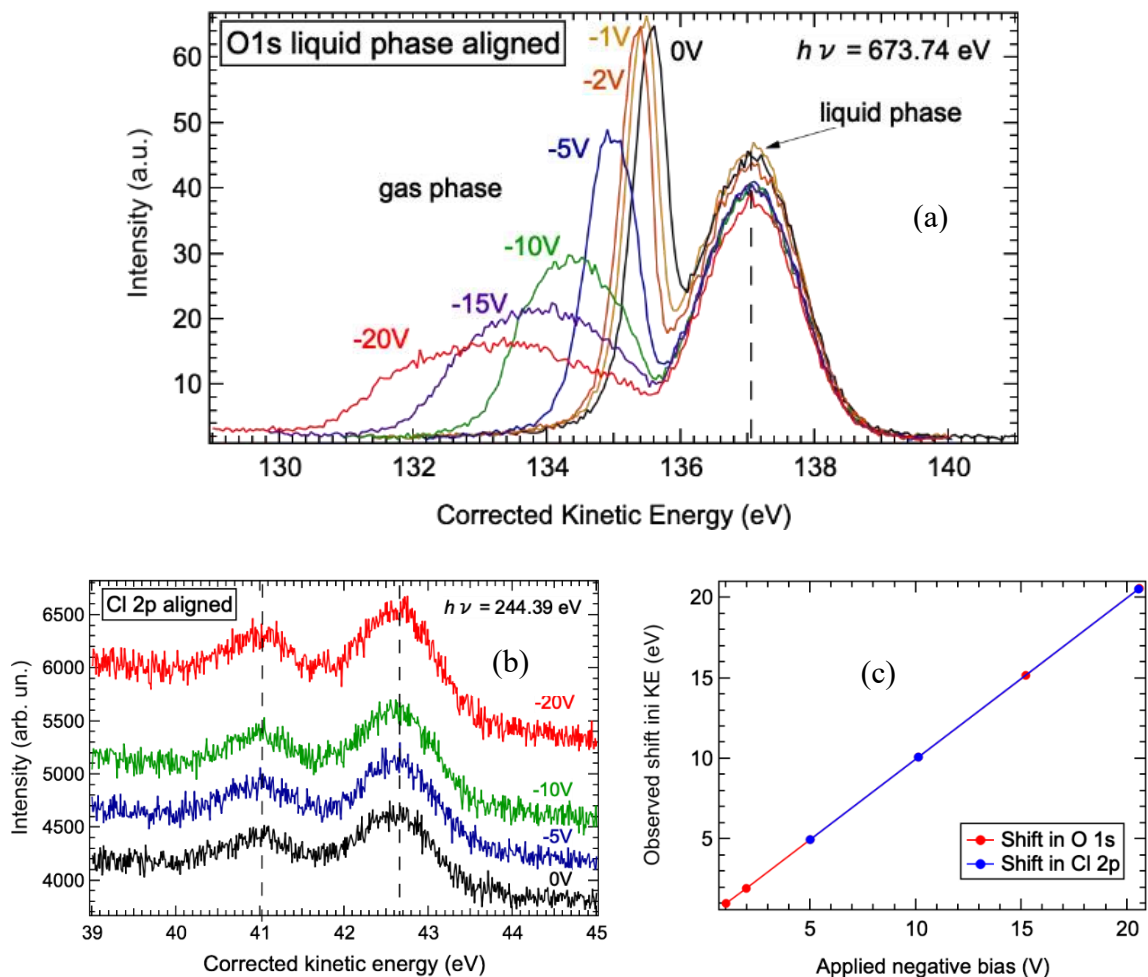


**Figure S4.** (a) O 1s core-level spectra of the 0.1 KCl solution under the effect of several values of  $V_{\text{bias}}$ . The spectra are aligned considering the nominal biases (given by the voltmeter). (b) Cl 2p core-level spectra of the 0.1 KCl solution aligned considering the nominal bias. (c) Observed KE shift versus nominal  $qV_{\text{bias}}$ .

Figure S4 (c) shows that the observed KE shift varies linearly (slope=1) with the nominal voltmeter  $qV_{\text{bias}}$ . However, at -20 V, we note a small difference between the voltmeter value and  $qV_{\text{bias}}$  deduced from XPS kinetic energy shifts. If due to an ohmic drop, this drop is small. For the KCl and Zobell solutions the applied nominal  $qV_{\text{bias}}$  is equal to 20.57 V while KE shift is 20.52 eV (0.05 eV smaller). For the  $\text{FeCl}_3/\text{FeCl}_2$  solution the nominal  $qV_{\text{bias}}$  was 20.00 eV, while the KE shift was 19.97 eV (0.03 eV smaller). The binding energies given in the main article are corrected from the XPS measured  $qV_{\text{bias}}$ .

## S6. The modified Helmholtz-Smoluchowski equation

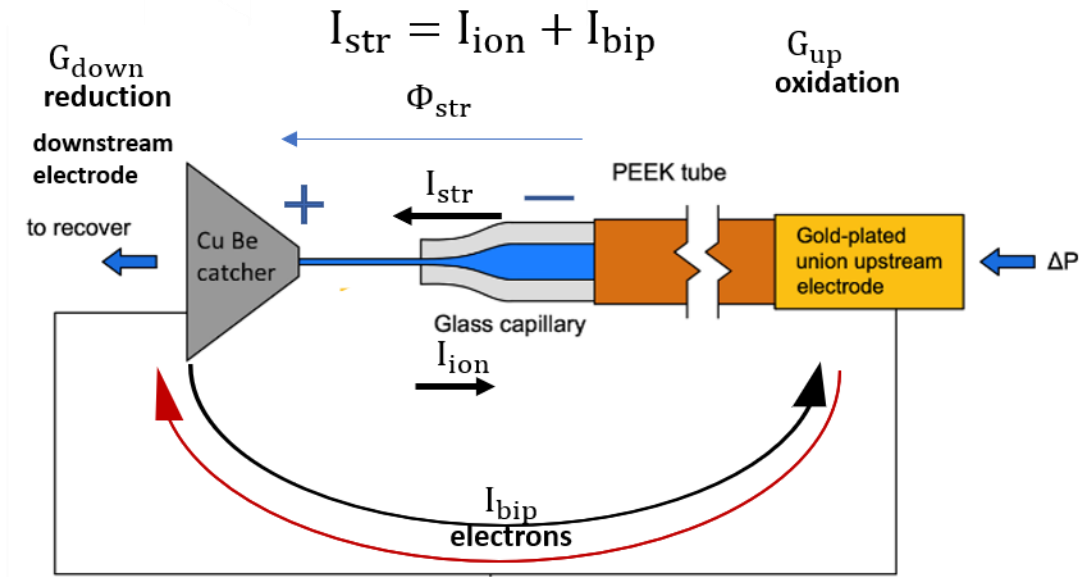


**Figure S5.** Schematics of the currents, assuming a bipolar faradaic process taking place at the upstream and downstream (catcher) electrodes.

The value of streaming current  $I_{str}$  observed in a capillary is usually related to the zeta ( $\zeta$ ) potential through the relation:<sup>10</sup>

$$I_{str} = \frac{\varepsilon \varepsilon_0 \zeta (\Delta p) S}{\eta L} \quad \{7\}$$

where  $\varepsilon$  is the relative dielectric constant of the solution,  $\varepsilon_0$  the vacuum permittivity,  $\zeta$  the zeta potential,  $\eta$  the dynamic viscosity of the solution,  $\Delta p$  the pressure difference before and after the capillary,  $S$  the section of the capillary and  $L$  its length.

The ionic conduction current in the capillary is:

$$I_{ion} = \frac{K_L S}{L} \Phi_{str} \quad \{8\}$$

where  $\Phi_{str}$  is the streaming potential, and  $K_L$  is the bulk solution conductivity (12.9 mS/cm).

The bipolar electronic current is:

$$I_{bip} = \frac{\Phi_{str}}{(G_{up}^{-1} + G_{down}^{-1})} \quad \{9\}$$

where  $G_{up}$  and  $G_{down}$  is the conductance of upstream jet/electrode junction and of the jet/catcher junction, respectively, in the presence of the redox species. At steady state, see Figure S5, the streaming current is equal to sum of the ionic conduction current and of the electronic bipolar current, therefore:

$$I_{str} = I_{ion} + I_{bip} \quad \{10\}$$

and combining relations {7} to {10} one obtains:

$$\phi_{str} = \frac{\frac{\epsilon\epsilon_0\zeta(\Delta p)S}{\eta L}}{\frac{K_L S}{L} + \frac{1}{(G_{up}^{-1} + G_{down}^{-1})}} \quad \{11\}$$

Increasing the solution conductivity (by addition of electrolytes) and the conductance at the upstream and downstream contact electrodes (by introducing a redox couple) diminishes  $\phi_{str}$ .

## S7. HOMO and SEEDC of the 0.1 M KCl solution

The valence and SEEDC spectra of the plain 0.1 M KCl solution are shown in Figure S6 and the fitting parameters are collected in Table S5.

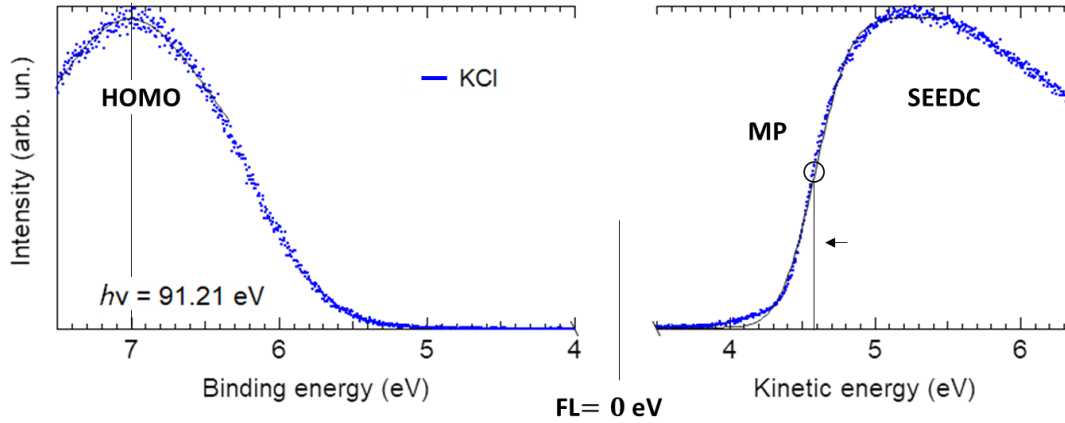


**Figure S6.** HOMO and SEEDC of the 0.1 M KCl solution (blue curve) and of the Zobell solution, referenced to the FL of the upward electrode/analyzer. The SEEDC rising edge is fitted using the erf function (black solid curve, see main article).

|   |           |
|---|-----------|
| measured $q\Phi$ (MP)                                     | 4.57(06)  |
| Width $\Gamma_{\text{SEEDC}}$                             | 0.45      |
| $q\Phi$ (onset)   | 4.34(06)  |
| $\text{BE}_{1b1(l)}$ centroid measured                    | 7.01(06)  |
| $\Gamma_{\text{HOMO}}$                                    | 1.39      |
| $\text{BE}_{1b1(\text{liq})}$ top (measured)              | 5.68      |
| $\text{IE}_{1b1(\text{liq})}$ 1b1 centroid to SEEDC MP    | 11.58(04) |
| $\text{IE}_{1b1(\text{liq})}$ 1b1 centroid to SEEDC onset | 11.34(04) |

**Table S5:** Fitting parameters of the HOMO and SEEDC curves of the plain 0.1 M KCl solution (all values are in eV)

## References

- 1 W. F. Egelhoff, *Surf. Sci. Rep.*, 1987, **6**, 253–415.
- 2 F. Ambrosio, Z. Guo and A. Pasquarello, *J. Phys. Chem. Lett.*, 2018, **9**, 3212–3216.
- 3 A. A. Isse and A. Gennaro, *J. Phys. Chem. B*, 2010, **114**, 7894–7899.
- 4 J. V. Coe, *Int. Rev. Phys. Chem.*, 2001, **20**, 33–58.
- 5 M. P. Seah, I. S. Gilmore and G. Beamson, *Surf. Interface Anal.*, 1998, **26**, 642–649.
- 6 C. Amatore, S. Arbault, E. Maisonhaute, S. Szunerits and L. Thouin, in *Trends in molecular electrochemistry*, eds. C. Amatore and A. Pombeiro, FontisMedia, Lausanne, 2004, pp. 385–411.
- 7 S. J. Konopka and B. McDuffie, *Anal. Chem.*, 1970, **42**, 1741–1746.
- 8 PHREEQC Version 3, <https://www.usgs.gov/software/phreeqc-version-3>, (accessed 31 December 2020).
- 9 N. Ottosson, M. Faubel, S. E. Bradforth, P. Jungwirth and B. Winter, *J. Electron Spectros. Relat. Phenomena*, 2010, **177**, 60–70.
- 10 A. V. Delgado, F. González-Caballero, R. J. Hunter, L. K. Koopal and J. Lyklema, *Pure Appl. Chem.*, 2005, **77**, 1753–1805.